

Signal processing on the sphere and applications

Jason McEwen

<http://www.jasonmcewen.org/>

*Institute of Electrical Engineering,
Ecole Polytechnique Fédérale de Lausanne (EPFL)*

*Department of Physics and Astronomy,
University College London (UCL)*

CaSP seminar :: Victoria University and IRL :: August 2011

Outline

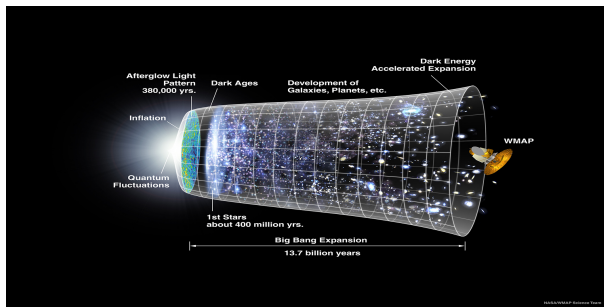
- 1 **Cosmology**
 - Big Bang
 - Cosmic microwave background
 - Observations
- 2 **Harmonic analysis on the sphere**
 - Spherical harmonic transform
 - Sampling theorems
- 3 **Wavelets on the sphere**
 - Why wavelets?
 - Continuous wavelets
 - Multiresolution analysis
- 4 **Applications**
 - Gaussianity of the CMB
 - Dark energy
 - Compression
 - Reflectance recovery

Outline

- 1 **Cosmology**
 - Big Bang
 - Cosmic microwave background
 - Observations
- 2 **Harmonic analysis on the sphere**
 - Spherical harmonic transform
 - Sampling theorems
- 3 **Wavelets on the sphere**
 - Why wavelets?
 - Continuous wavelets
 - Multiresolution analysis
- 4 **Applications**
 - Gaussianity of the CMB
 - Dark energy
 - Compression
 - Reflectance recovery

Cosmological concordance model

- **Concordance model of modern cosmology** emerged recently with many cosmological parameters constrained to high precision.
- General description is of a Universe undergoing accelerated expansion, containing 4% ordinary baryonic matter, 22% cold dark matter and 74% dark energy.
- Structure and evolution of the Universe constrained through cosmological observations.



Credit: WMAP Science Team

Cosmic microwave background (CMB)

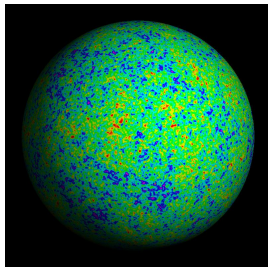
- Temperature of early Universe sufficiently hot that **photons** had enough energy to **ionise hydrogen**.
- Compton scattering happened frequently \Rightarrow **mean free path of photons extremely small**.
- Universe consisted of an **opaque photon-baryon fluid**.
- **As Universe expanded it cooled**, until majority of photons no longer had sufficient energy to ionise hydrogen.
- Photons decoupled from baryons and the **Universe became essentially transparent to radiation**.
- *Recombination* occurred when temperature of Universe dropped to 3000K ($\sim 400,000$ years after the Big Bang).
- Photons then free to propagate largely unhindered and observed today on **celestial sphere** as **CMB radiation**.
- CMB is highly uniform over the celestial sphere, however it contains **small fluctuations** at a relative level of 10^{-5} due to acoustic oscillations in the early Universe.
- CMB **observed on spherical manifold**, hence the geometry of the sphere must be taken into account in any analysis.

Cosmic microwave background (CMB)

- Temperature of early Universe sufficiently hot that **photons** had enough energy to **ionise hydrogen**.
- Compton scattering happened frequently \Rightarrow **mean free path of photons extremely small**.
- Universe consisted of an **opaque photon-baryon fluid**.
- **As Universe expanded it cooled**, until majority of photons no longer had sufficient energy to ionise hydrogen.
- Photons decoupled from baryons and the **Universe became essentially transparent to radiation**.
- *Recombination* occurred when temperature of Universe dropped to 3000K ($\sim 400,000$ years after the Big Bang).
- Photons then free to propagate largely unhindered and observed today on **celestial sphere** as **CMB radiation**.
- CMB is highly uniform over the celestial sphere, however it contains **small fluctuations** at a relative level of 10^{-5} due to acoustic oscillations in the early Universe.
- CMB **observed on spherical manifold**, hence the geometry of the sphere must be taken into account in any analysis.

Cosmic microwave background (CMB)

- Temperature of early Universe sufficiently hot that **photons** had enough energy to **ionise hydrogen**.
- Compton scattering happened frequently \Rightarrow **mean free path of photons extremely small**.
- Universe consisted of an **opaque photon-baryon fluid**.
- **As Universe expanded it cooled**, until majority of photons no longer had sufficient energy to ionise hydrogen.
- Photons decoupled from baryons and the **Universe became essentially transparent to radiation**.
- *Recombination* occurred when temperature of Universe dropped to 3000K ($\sim 400,000$ years after the Big Bang).
- Photons then free to propagate largely unhindered and observed today on **celestial sphere** as **CMB radiation**.
- CMB is highly uniform over the celestial sphere, however it contains **small fluctuations** at a relative level of 10^{-5} due to acoustic oscillations in the early Universe.
- CMB **observed on spherical manifold**, hence the geometry of the sphere must be taken into account in any analysis.



Credit: Max Tegmark

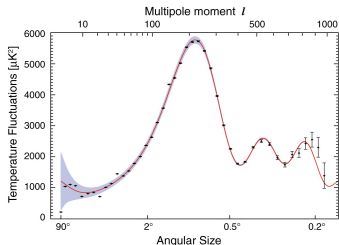
Cosmic microwave background (CMB)

- Quantum fluctuations in the early Universe blown to macroscopic scales by inflation, establishing acoustic oscillations in primordial plasma of the very early Universe.
- Provide the **seeds of structure formation** in our Universe.
- Cosmological concordance model explains the power spectrum of these oscillations to very high precision.

- Although a general cosmological concordance model is now established, many details remain unclear. Study of **more exotic cosmological models** now important.

Cosmic microwave background (CMB)

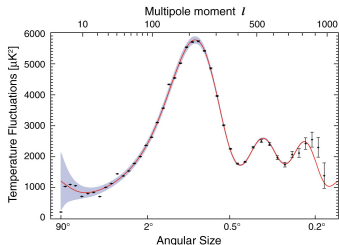
- Quantum fluctuations in the early Universe blown to macroscopic scales by inflation, establishing acoustic oscillations in primordial plasma of the very early Universe.
- Provide the **seeds of structure formation** in our Universe.
- Cosmological concordance model explains the power spectrum of these oscillations to very high precision.



- Although a general cosmological concordance model is now established, many details remain unclear. Study of **more exotic cosmological models** now important.

Cosmic microwave background (CMB)

- Quantum fluctuations in the early Universe blown to macroscopic scales by inflation, establishing acoustic oscillations in primordial plasma of the very early Universe.
- Provide the **seeds of structure formation** in our Universe.
- Cosmological concordance model explains the power spectrum of these oscillations to very high precision.



Credit: WMAP Science Team

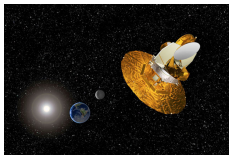
- Although a general cosmological concordance model is now established, many details remain unclear. Study of **more exotic cosmological models** now important.

Observations of the CMB

- Full-sky observations of the CMB ongoing.



(a) COBE (launched 1989)



(b) WMAP (launched 2001)



(c) Planck (launched 2009)

Figure: Full-sky CMB observations

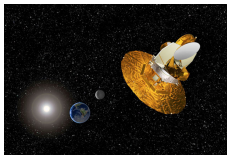
- Each new experiment provides dramatic improvement in precision and resolution of observations (e.g. COBE to WMAP illustration).

Observations of the CMB

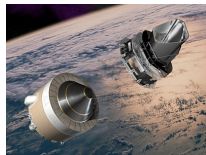
- Full-sky observations of the CMB ongoing.



(a) COBE (launched 1989)



(b) WMAP (launched 2001)



(c) Planck (launched 2009)

Figure: Full-sky CMB observations

- Each new experiment provides dramatic improvement in precision and resolution of observations (e.g. COBE to WMAP illustration).

(cobe 2 wmap movie)

Credit: WMAP Science Team

Outline

- 1 Cosmology
 - Big Bang
 - Cosmic microwave background
 - Observations
- 2 Harmonic analysis on the sphere
 - Spherical harmonic transform
 - Sampling theorems
- 3 Wavelets on the sphere
 - Why wavelets?
 - Continuous wavelets
 - Multiresolution analysis
- 4 Applications
 - Gaussianity of the CMB
 - Dark energy
 - Compression
 - Reflectance recovery

Spherical harmonics

- Consider the **space of square integrable functions on the sphere** $L^2(S^2)$, with the **inner product** of $f, g \in L^2(S^2)$ defined by

$$\langle f, g \rangle = \int_{S^2} d\Omega(\theta, \varphi) f(\theta, \varphi) g^*(\theta, \varphi),$$

where $d\Omega(\theta, \varphi) = \sin \theta d\theta d\varphi$ is the usual invariant measure on the sphere and (θ, φ) define spherical coordinates with colatitude $\theta \in [0, \pi]$ and longitude $\varphi \in [0, 2\pi)$. Complex conjugation is denoted by the superscript $*$.

- The scalar **spherical harmonic** functions form the **canonical orthogonal basis** for the space of $L^2(S^2)$ scalar functions on the sphere and are defined by

$$Y_{\ell m}(\theta, \varphi) = \sqrt{\frac{2\ell + 1}{4\pi} \frac{(\ell - m)!}{(\ell + m)!}} P_{\ell}^m(\cos \theta) e^{im\varphi},$$

for natural $\ell \in \mathbb{N}$ and integer $m \in \mathbb{Z}$, $|m| \leq \ell$, where $P_{\ell}^m(x)$ are the associated Legendre functions.

- Eigenfunctions of the Laplacian on the sphere: $\Delta_{S^2} Y_{\ell m} = -\ell(\ell + 1)Y_{\ell m}$.
- Orthogonality relation: $\langle Y_{\ell m}, Y_{\ell' m'} \rangle = \delta_{\ell\ell'} \delta_{mm'}$, where δ_{ij} is the Kronecker delta symbol.
- Completeness relation:

$$\sum_{\ell=0}^{\infty} \sum_{m=-\ell}^{\ell} Y_{\ell m}(\theta, \varphi) Y_{\ell m}^*(\theta', \varphi') = \delta(\cos \theta - \cos \theta') \delta(\varphi - \varphi'),$$

where $\delta(x)$ is the Dirac delta function.

Spherical harmonics

- Consider the **space of square integrable functions on the sphere** $L^2(S^2)$, with the **inner product** of $f, g \in L^2(S^2)$ defined by

$$\langle f, g \rangle = \int_{S^2} d\Omega(\theta, \varphi) f(\theta, \varphi) g^*(\theta, \varphi),$$

where $d\Omega(\theta, \varphi) = \sin \theta d\theta d\varphi$ is the usual invariant measure on the sphere and (θ, φ) define spherical coordinates with colatitude $\theta \in [0, \pi]$ and longitude $\varphi \in [0, 2\pi)$. Complex conjugation is denoted by the superscript $*$.

- The scalar **spherical harmonic** functions form the **canonical orthogonal basis** for the space of $L^2(S^2)$ scalar functions on the sphere and are defined by

$$Y_{\ell m}(\theta, \varphi) = \sqrt{\frac{2\ell + 1}{4\pi} \frac{(\ell - m)!}{(\ell + m)!}} P_{\ell}^m(\cos \theta) e^{im\varphi},$$

for natural $\ell \in \mathbb{N}$ and integer $m \in \mathbb{Z}$, $|m| \leq \ell$, where $P_{\ell}^m(x)$ are the associated Legendre functions.

- Eigenfunctions of the Laplacian on the sphere: $\Delta_{S^2} Y_{\ell m} = -\ell(\ell + 1)Y_{\ell m}$.
- Orthogonality relation: $\langle Y_{\ell m}, Y_{\ell' m'} \rangle = \delta_{\ell\ell'} \delta_{mm'}$, where δ_{ij} is the Kronecker delta symbol.
- Completeness relation:

$$\sum_{\ell=0}^{\infty} \sum_{m=-\ell}^{\ell} Y_{\ell m}(\theta, \varphi) Y_{\ell m}^*(\theta', \varphi') = \delta(\cos \theta - \cos \theta') \delta(\varphi - \varphi'),$$

where $\delta(x)$ is the Dirac delta function.

Spherical harmonics

- Consider the **space of square integrable functions on the sphere** $L^2(S^2)$, with the **inner product** of $f, g \in L^2(S^2)$ defined by

$$\langle f, g \rangle = \int_{S^2} d\Omega(\theta, \varphi) f(\theta, \varphi) g^*(\theta, \varphi),$$

where $d\Omega(\theta, \varphi) = \sin \theta d\theta d\varphi$ is the usual invariant measure on the sphere and (θ, φ) define spherical coordinates with colatitude $\theta \in [0, \pi]$ and longitude $\varphi \in [0, 2\pi)$. Complex conjugation is denoted by the superscript $*$.

- The scalar **spherical harmonic** functions form the **canonical orthogonal basis** for the space of $L^2(S^2)$ scalar functions on the sphere and are defined by

$$Y_{\ell m}(\theta, \varphi) = \sqrt{\frac{2\ell + 1}{4\pi} \frac{(\ell - m)!}{(\ell + m)!}} P_{\ell}^m(\cos \theta) e^{im\varphi},$$

for natural $\ell \in \mathbb{N}$ and integer $m \in \mathbb{Z}$, $|m| \leq \ell$, where $P_{\ell}^m(x)$ are the associated Legendre functions.

- Eigenfunctions of the Laplacian on the sphere: $\Delta_{S^2} Y_{\ell m} = -\ell(\ell + 1)Y_{\ell m}$.
- Orthogonality relation: $\langle Y_{\ell m}, Y_{\ell' m'} \rangle = \delta_{\ell\ell'} \delta_{mm'}$, where δ_{ij} is the Kronecker delta symbol.
- Completeness relation:

$$\sum_{\ell=0}^{\infty} \sum_{m=-\ell}^{\ell} Y_{\ell m}(\theta, \varphi) Y_{\ell m}^*(\theta', \varphi') = \delta(\cos \theta - \cos \theta') \delta(\varphi - \varphi'),$$

where $\delta(x)$ is the Dirac delta function.

Spherical harmonic transform

- Any square integrable scalar function on the sphere $f \in L^2(S^2)$ may be represented by its **spherical harmonic expansion**:

$$f(\theta, \varphi) = \sum_{\ell=0}^{\infty} \sum_{m=-\ell}^{\ell} f_{\ell m} Y_{\ell m}(\theta, \varphi).$$

- The **spherical harmonic coefficients** are given by the usual projection onto each basis function:

$$f_{\ell m} = \langle f, Y_{\ell m} \rangle.$$

- We consider signals on the sphere **band-limited** at L , that is signals such that $f_{\ell m} = 0, \forall \ell \geq L$
 \Rightarrow summations may be truncated at $L - 1$.
- For a band-limited signal, can we compute $f_{\ell m}$ exactly?
 \rightarrow **Sampling theorems on the sphere!**
- Aside: Generalise to spin functions on the sphere.

Square integrable spin functions on the sphere $s_f \in L^2(S^2)$, with integer spin $s \in \mathbb{Z}$, are defined by their behaviour under local rotations. By definition, a spin function transforms as

$$s_f'(\theta, \varphi) = e^{-is\chi} s_f(\theta, \varphi)$$

under a local rotation by χ , where the prime denotes the rotated function.

Spherical harmonic transform

- Any square integrable scalar function on the sphere $f \in L^2(S^2)$ may be represented by its **spherical harmonic expansion**:

$$f(\theta, \varphi) = \sum_{\ell=0}^{\infty} \sum_{m=-\ell}^{\ell} f_{\ell m} Y_{\ell m}(\theta, \varphi).$$

- The **spherical harmonic coefficients** are given by the usual projection onto each basis function:

$$f_{\ell m} = \langle f, Y_{\ell m} \rangle.$$

- We consider signals on the sphere **band-limited** at L , that is signals such that $f_{\ell m} = 0, \forall \ell \geq L$
 \Rightarrow summations may be truncated at $L - 1$.
- For a band-limited signal, can we compute $f_{\ell m}$ exactly?
 \rightarrow **Sampling theorems on the sphere!**
- Aside: Generalise to spin functions on the sphere.

Square integrable spin functions on the sphere $s_f \in L^2(S^2)$, with integer spin $s \in \mathbb{Z}$, are defined by their behaviour under local rotations. By definition, a spin function transforms as

$$s_f'(\theta, \varphi) = e^{-is\chi} s_f(\theta, \varphi)$$

under a local rotation by χ , where the prime denotes the rotated function.

Spherical harmonic transform

- Any square integrable scalar function on the sphere $f \in L^2(S^2)$ may be represented by its **spherical harmonic expansion**:

$$f(\theta, \varphi) = \sum_{\ell=0}^{\infty} \sum_{m=-\ell}^{\ell} f_{\ell m} Y_{\ell m}(\theta, \varphi).$$

- The **spherical harmonic coefficients** are given by the usual projection onto each basis function:

$$f_{\ell m} = \langle f, Y_{\ell m} \rangle.$$

- We consider signals on the sphere **band-limited** at L , that is signals such that $f_{\ell m} = 0, \forall \ell \geq L$
 \Rightarrow summations may be truncated at $L - 1$.
- For a band-limited signal, can we compute $f_{\ell m}$ exactly?
 \rightarrow **Sampling theorems on the sphere!**
- Aside: Generalise to spin functions on the sphere.

Square integrable spin functions on the sphere $s f \in L^2(S^2)$, with integer spin $s \in \mathbb{Z}$, are defined by their behaviour under local rotations. By definition, a spin function transforms as

$$s f'(\theta, \varphi) = e^{-is\chi} s f(\theta, \varphi)$$

under a local rotation by χ , where the prime denotes the rotated function.

Spherical harmonic transform

- Any square integrable scalar function on the sphere $f \in L^2(S^2)$ may be represented by its **spherical harmonic expansion**:

$$f(\theta, \varphi) = \sum_{\ell=0}^{\infty} \sum_{m=-\ell}^{\ell} f_{\ell m} Y_{\ell m}(\theta, \varphi).$$

- The **spherical harmonic coefficients** are given by the usual projection onto each basis function:

$$f_{\ell m} = \langle f, Y_{\ell m} \rangle.$$

- We consider signals on the sphere **band-limited** at L , that is signals such that $f_{\ell m} = 0, \forall \ell \geq L$
 \Rightarrow summations may be truncated at $L - 1$.
- For a band-limited signal, can we compute $f_{\ell m}$ exactly?
 \rightarrow **Sampling theorems on the sphere!**
- Aside: Generalise to spin functions on the sphere.

Square integrable spin functions on the sphere ${}_s f \in L^2(S^2)$, with integer spin $s \in \mathbb{Z}$, are defined by their behaviour under local rotations. By definition, a spin function transforms as

$${}_s f'(\theta, \varphi) = e^{-is\chi} {}_s f(\theta, \varphi)$$

under a local rotation by χ , where the prime denotes the rotated function.

Sampling theorems on the sphere: state-of-the-art

- In-exact spherical harmonic transforms exist for a variety of pixelisations of the sphere.
 - HEALpix (Gorski *et al.* 2005)
 - IGLOO (Crittenden & Turok 1998)

→ Do NOT lead to sampling theorems on the sphere!
- Driscoll & Healy (1994) sampling theorem
 - Equiangular pixelisation of the sphere
 - Require $\sim 4L^2$ samples on the sphere
 - Semi-naive algorithm with complexity $O(L^3)$
(algorithms with lower scaling exist but they are not generally stable)
 - Require a precomputation or otherwise restricted use of Wigner recursions
- Gauss-Legendre sampling theorem
 - Not generally so well-know (no published work)
 - Sample positions given by roots of Legendre functions
 - Require $\sim 2L^2$ samples on the sphere
 - Simple separation of variables gives algorithm with complexity $O(L^3)$
 - Require a precomputation or otherwise restricted use of Wigner recursions

Sampling theorems on the sphere: state-of-the-art

- In-exact spherical harmonic transforms exist for a variety of pixelisations of the sphere.
 - HEALpix (Gorski *et al.* 2005)
 - IGLOO (Crittenden & Turok 1998)

→ Do NOT lead to sampling theorems on the sphere!
- Driscoll & Healy (1994) sampling theorem
 - Equiangular pixelisation of the sphere
 - Require $\sim 4L^2$ samples on the sphere
 - Semi-naive algorithm with complexity $\mathcal{O}(L^3)$
(algorithms with lower scaling exist but they are not generally stable)
 - Require a precomputation or otherwise restricted use of Wigner recursions
- Gauss-Legendre sampling theorem
 - Not generally so well-know (no published work)
 - Sample positions given by roots of Legendre functions
 - Require $\sim 2L^2$ samples on the sphere
 - Simple separation of variables gives algorithm with complexity $\mathcal{O}(L^3)$
 - Require a precomputation or otherwise restricted use of Wigner recursions

Sampling theorems on the sphere: state-of-the-art

- In-exact spherical harmonic transforms exist for a variety of pixelisations of the sphere.
 - HEALpix (Gorski *et al.* 2005)
 - IGLOO (Crittenden & Turok 1998)

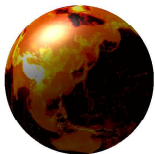
→ Do NOT lead to sampling theorems on the sphere!
- Driscoll & Healy (1994) sampling theorem
 - Equiangular pixelisation of the sphere
 - Require $\sim 4L^2$ samples on the sphere
 - Semi-naive algorithm with complexity $\mathcal{O}(L^3)$
(algorithms with lower scaling exist but they are not generally stable)
 - Require a precomputation or otherwise restricted use of Wigner recursions
- Gauss-Legendre sampling theorem
 - Not generally so well-know (no published work)
 - Sample positions given by roots of Legendre functions
 - Require $\sim 2L^2$ samples on the sphere
 - Simple separation of variables gives algorithm with complexity $\mathcal{O}(L^3)$
 - Require a precomputation or otherwise restricted use of Wigner recursions

Sampling theorems on the sphere: a novel sampling theorem

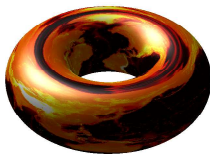
- We have developed a **new sampling theorem and corresponding fast algorithms** by performing a factoring of rotations and then by associating the sphere with the torus through a periodic extension.
- Similar (in flavour but not detail!) to making a periodic extension in θ of a function f on the sphere.

Sampling theorems on the sphere: a novel sampling theorem

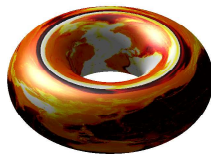
- We have developed a **new sampling theorem and corresponding fast algorithms** by performing a factoring of rotations and then by associating the sphere with the torus through a periodic extension.
- Similar (in flavour but not detail!) to making a periodic extension in θ of a function f on the sphere.



(a) Function on sphere



(b) Even function on torus



(c) Odd function on torus

Figure: Associating functions on the sphere and torus

Sampling theorems on the sphere: a novel sampling theorem

- By a factoring of rotations (Wigner decomposition), a reordering of summations and a separation of variables, the **inverse transform** of f may be written:

Inverse spherical harmonic transform

$$sf(\theta, \varphi) = \sum_{m=-(L-1)}^{L-1} {}_sF_m(\theta) e^{im\varphi}$$

$${}_sF_m(\theta) = \sum_{m'=-L+1}^{L-1} {}_sF_{mm'} e^{im'\theta}$$

$${}_sF_{mm'} = (-1)^s i^{-(m+s)} \sum_{\ell=0}^{L-1} \sqrt{\frac{2\ell+1}{4\pi}} \Delta_{m'm}^{\ell} \Delta_{m',-s}^{\ell} {}_s f_{\ell m}$$

where $\Delta_{mn}^{\ell} \equiv d_{mn}^{\ell}(\pi/2)$ are the reduced Wigner functions evaluated at $\pi/2$.

Sampling theorems on the sphere: a novel sampling theorem

- By a factoring of rotations (Wigner decomposition), a reordering of summations and a separation of variables, the **forward transform** of ${}_s f$ may be written:

Forward spherical harmonic transform

$${}_s f_{\ell m} = (-1)^s i^{m+s} \sqrt{\frac{2\ell+1}{4\pi}} \sum_{m'=-\ell}^{\ell} \Delta_{m'm}^{\ell} \Delta_{m',-s}^{\ell} {}_s G_{mm'}$$

$${}_s G_{mm'} = \int_0^{\pi} d\theta \sin \theta {}_s G_m(\theta) e^{-im'\theta}$$

$${}_s G_m(\theta) = \int_0^{2\pi} d\varphi {}_s f(\theta, \varphi) e^{-im\varphi}$$

- Recasting the forward and inverse spherical harmonic transforms in this manner is no more efficient or accurate than the original formulation.
- However, it **highlights similarities with Fourier series** representations and reduces the problem of finding an exact quadrature rule to the calculation of ${}_s G_{mm'}$ only.
- The Fourier series expansion is only defined for periodic functions; thus, to recast these expressions in a form amenable to the application of Fourier transforms we must make a **periodic extension** in colatitude θ .

Sampling theorems on the sphere: a novel sampling theorem

- By a factoring of rotations (Wigner decomposition), a reordering of summations and a separation of variables, the **forward transform** of ${}_s f$ may be written:

Forward spherical harmonic transform

$${}_s f_{\ell m} = (-1)^s i^{m+s} \sqrt{\frac{2\ell+1}{4\pi}} \sum_{m'=-\ell}^{\ell} \Delta_{m' m}^{\ell} \Delta_{m', -s}^{\ell} {}_s G_{mm'}$$

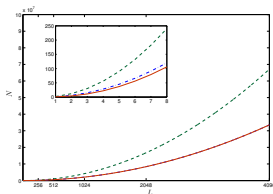
$${}_s G_{mm'} = \int_0^{\pi} d\theta \sin \theta {}_s G_m(\theta) e^{-im'\theta}$$

$${}_s G_m(\theta) = \int_0^{2\pi} d\varphi {}_s f(\theta, \varphi) e^{-im\varphi}$$

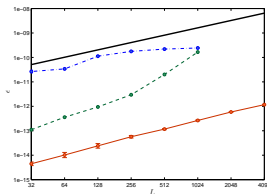
- Recasting the forward and inverse spherical harmonic transforms in this manner is no more efficient or accurate than the original formulation.
- However, it **highlights similarities with Fourier series** representations and reduces the problem of finding an exact quadrature rule to the calculation of ${}_s G_{mm'}$ only.
- The Fourier series expansion is only defined for periodic functions; thus, to recast these expressions in a form amenable to the application of Fourier transforms we must make a **periodic extension** in colatitude θ .

Sampling theorems on the sphere: a novel sampling theorem

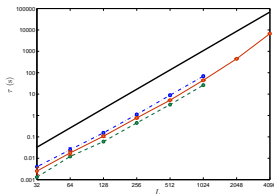
- Properties of our new sampling theorem
 - **Equiangular pixelisation** of the sphere
 - Require $\sim 2L^2$ **samples** on the sphere (and still fewer than Gauss-Legendre sampling)
 - Exploit fast Fourier transforms to yield a **fast algorithm** with complexity $\mathcal{O}(L^3)$
 - **No precomputation** and **very flexible regarding use of Wigner recursions**
 - Extends to **spin function** on the sphere with no change in complexity or computation time



(a) Number of samples



(b) Numerical accuracy



(c) Computation time

Figure: Performance of our sampling theorem (MW=red; DH=green; Gauss-Legendre=blue)

Outline

- 1 Cosmology
 - Big Bang
 - Cosmic microwave background
 - Observations
- 2 Harmonic analysis on the sphere
 - Spherical harmonic transform
 - Sampling theorems
- 3 Wavelets on the sphere
 - Why wavelets?
 - Continuous wavelets
 - Multiresolution analysis
- 4 Applications
 - Gaussianity of the CMB
 - Dark energy
 - Compression
 - Reflectance recovery

Why wavelets?



Fourier (1807)



Haar (1909)

Morlet and Grossman (1981)

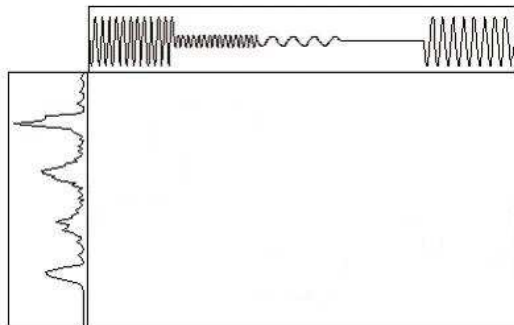


Figure: Fourier vs wavelet transform (image from <http://www.wavelet.org/tutorial/>)

Why wavelets?



Fourier (1807)



Haar (1909)

Morlet and Grossman (1981)

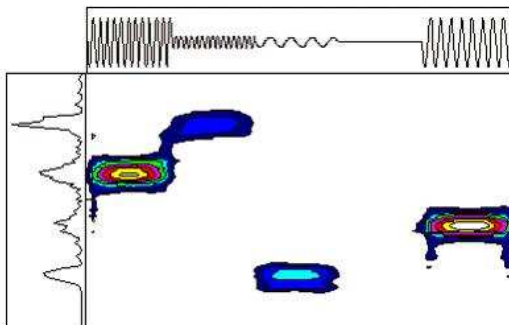


Figure: Fourier vs wavelet transform (image from <http://www.wavelet.org/tutorial/>)

Recall wavelet transform in Euclidean space

- Project signal onto wavelets

$$\mathcal{W}^f(a, b) = \langle f, \psi_{a,b} \rangle = |a|^{-1/2} \int_{-\infty}^{\infty} dt f(t) \psi^* \left(\frac{t-b}{a} \right),$$

where $\psi_{a,b} = |a|^{-1/2} \psi \left(\frac{t-b}{a} \right)$.

- Synthesis signal from wavelet coefficients

$$f(t) = C_{\psi}^{-1} \int_{-\infty}^{\infty} db \int_0^{\infty} \frac{da}{a^2} \mathcal{W}^f(a, b) \psi_{a,b}(t).$$

- Admissibility condition to ensure perfect reconstruction

$$0 < C_{\psi} \equiv \int_{-\infty}^{\infty} \frac{dk}{|k|} |\hat{\psi}(k)|^2 < \infty.$$

- Construct on sphere in analogous manner.

Wavelets on the sphere

- Follow construction derived by Antoine and Vandergheynst (1998) (reintroduced by Wiaux (2005)).
- Construct **wavelet atoms from affine transformations** (dilation, translation) on the sphere of a mother wavelet.
- The natural **extension of translations to the sphere are rotations**. Characterised by the elements of the rotation group $SO(3)$, which parameterise in terms of the three Euler angles $\rho = (\alpha, \beta, \gamma)$. Rotation of a function f on the sphere is defined by

$$[\mathcal{R}(\rho)f](\omega) = f(\rho^{-1}\omega), \quad \rho \in SO(3).$$

- **How define dilation and admissible wavelets on the sphere?**

Wavelets on the sphere

- Follow construction derived by Antoine and Vandergheynst (1998) (reintroduced by Wiaux (2005)).
- Construct **wavelet atoms from affine transformations** (dilation, translation) on the sphere of a mother wavelet.
- The natural **extension of translations to the sphere are rotations**. Characterised by the elements of the rotation group $SO(3)$, which parameterise in terms of the three Euler angles $\rho = (\alpha, \beta, \gamma)$. Rotation of a function f on the sphere is defined by

$$[\mathcal{R}(\rho)f](\omega) = f(\rho^{-1}\omega), \quad \rho \in SO(3).$$

- How define dilation and admissible wavelets on the sphere?

Wavelets on the sphere

- Follow construction derived by Antoine and Vandergheynst (1998) (reintroduced by Wiaux (2005)).
- Construct **wavelet atoms from affine transformations** (dilation, translation) on the sphere of a mother wavelet.
- The natural **extension of translations to the sphere are rotations**. Characterised by the elements of the rotation group $SO(3)$, which parameterise in terms of the three Euler angles $\rho = (\alpha, \beta, \gamma)$. Rotation of a function f on the sphere is defined by

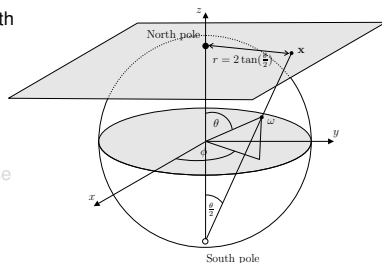
$$[\mathcal{R}(\rho)f](\omega) = f(\rho^{-1}\omega), \quad \rho \in SO(3).$$

- **How define dilation and admissible wavelets on the sphere?**

Stereographic projection

- Apply **stereographic projection** to build an association with the plane.

- Stereographic projection operator is defined by $\Pi : \omega \rightarrow x = \Pi\omega = (r(\theta), \varphi)$ where $r = 2 \tan(\theta/2)$, $\omega \equiv (\theta, \varphi) \in S^2$ and $x \in \mathbb{R}^2$ is a point in the plane, denoted here by the polar coordinates (r, φ) . The inverse operator is $\Pi^{-1} : x \rightarrow \omega = \Pi^{-1}x = (\theta(r), \varphi)$, where $\theta(r) = 2 \tan^{-1}(r/2)$.



- Define the **action** of the stereographic projection operator **on functions** on the plane and sphere. Consider the space of square integrable functions in $L^2(\mathbb{R}^2, d^2x)$ on the plane and $L^2(S^2, d\Omega(\omega))$ on the sphere.

- The action of the **stereographic projection operator** $\Pi : f \in L^2(S^2, d\Omega(\omega)) \rightarrow p = \Pi f \in L^2(\mathbb{R}^2, d^2x)$ on functions is defined as

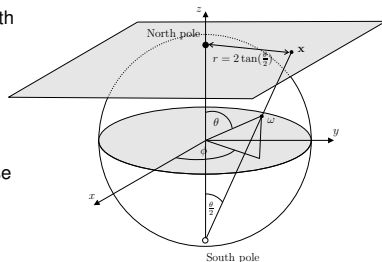
$$p(r, \varphi) = (\Pi f)(r, \varphi) = (1 + r^2/4)^{-1} f(\theta(r), \varphi) .$$

- The **inverse stereographic projection operator** $\Pi^{-1} : p \in L^2(\mathbb{R}^2, d^2x) \rightarrow f = \Pi^{-1}p \in L^2(S^2, d\Omega(\omega))$ on functions is then

$$f(\theta, \varphi) = (\Pi^{-1}p)(\theta, \varphi) = [1 + \tan^2(\theta/2)] p(r(\theta), \varphi) .$$

Stereographic projection

- Apply **stereographic projection** to build an association with the plane.
- Stereographic projection operator is defined by $\Pi : \omega \rightarrow \mathbf{x} = \Pi\omega = (r(\theta), \varphi)$ where $r = 2 \tan(\theta/2)$, $\omega \equiv (\theta, \varphi) \in S^2$ and $\mathbf{x} \in \mathbb{R}^2$ is a point in the plane, denoted here by the polar coordinates (r, φ) . The inverse operator is $\Pi^{-1} : \mathbf{x} \rightarrow \omega = \Pi^{-1}\mathbf{x} = (\theta(r), \varphi)$, where $\theta(r) = 2 \tan^{-1}(r/2)$.



- Define the **action** of the stereographic projection operator **on functions** on the plane and sphere. Consider the space of square integrable functions in $L^2(\mathbb{R}^2, d^2x)$ on the plane and $L^2(S^2, d\Omega(\omega))$ on the sphere.

- The action of the **stereographic projection operator** $\Pi : f \in L^2(S^2, d\Omega(\omega)) \rightarrow p = \Pi f \in L^2(\mathbb{R}^2, d^2x)$ on functions is defined as

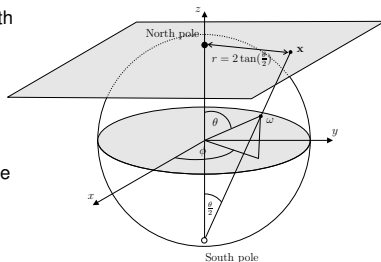
$$p(r, \varphi) = (\Pi f)(r, \varphi) = (1 + r^2/4)^{-1} f(\theta(r), \varphi).$$

- The **inverse stereographic projection operator** $\Pi^{-1} : p \in L^2(\mathbb{R}^2, d^2x) \rightarrow f = \Pi^{-1} p \in L^2(S^2, d\Omega(\omega))$ on functions is then

$$f(\theta, \varphi) = (\Pi^{-1} p)(\theta, \varphi) = [1 + \tan^2(\theta/2)] p(r(\theta), \varphi).$$

Stereographic projection

- Apply **stereographic projection** to build an association with the plane.
- Stereographic projection operator is defined by $\Pi : \omega \rightarrow \mathbf{x} = \Pi\omega = (r(\theta), \varphi)$ where $r = 2 \tan(\theta/2)$, $\omega \equiv (\theta, \varphi) \in S^2$ and $\mathbf{x} \in \mathbb{R}^2$ is a point in the plane, denoted here by the polar coordinates (r, φ) . The inverse operator is $\Pi^{-1} : \mathbf{x} \rightarrow \omega = \Pi^{-1}\mathbf{x} = (\theta(r), \varphi)$, where $\theta(r) = 2 \tan^{-1}(r/2)$.



- Define the **action** of the stereographic projection operator **on functions** on the plane and sphere. Consider the space of square integrable functions in $L^2(\mathbb{R}^2, d^2\mathbf{x})$ on the plane and $L^2(S^2, d\Omega(\omega))$ on the sphere.

- The action of the **stereographic projection operator** $\Pi : f \in L^2(S^2, d\Omega(\omega)) \rightarrow p = \Pi f \in L^2(\mathbb{R}^2, d^2\mathbf{x})$ on functions is defined as

$$p(r, \varphi) = (\Pi f)(r, \varphi) = (1 + r^2/4)^{-1} f(\theta(r), \varphi).$$

- The **inverse stereographic projection operator** $\Pi^{-1} : p \in L^2(\mathbb{R}^2, d^2\mathbf{x}) \rightarrow f = \Pi^{-1} p \in L^2(S^2, d\Omega(\omega))$ on functions is then

$$f(\theta, \varphi) = (\Pi^{-1} p)(\theta, \varphi) = [1 + \tan^2(\theta/2)] p(r(\theta), \varphi).$$

Dilation on the sphere

- The **spherical dilation operator** $\mathcal{D}(a) : f(\omega) \rightarrow [\mathcal{D}(a)f](\omega)$ in $L^2(S^2, d\Omega(\omega))$ is defined as the conjugation by Π of the Euclidean dilation $d(a)$ in $L^2(\mathbb{R}^2, d^2\mathbf{x})$ on tangent plane at north pole:

$$\mathcal{D}(a) \equiv \Pi^{-1} d(a) \Pi .$$

- Spherical dilation given by

$$[\mathcal{D}(a)f](\omega) = [\lambda(a, \theta, \varphi)]^{1/2} f(\omega_{1/a}) ,$$

where $\omega_a = (\theta_a, \varphi)$ and $\tan(\theta_a/2) = a \tan(\theta/2)$.

- Cocycle of a spherical dilation is defined by

$$\lambda(a, \theta, \varphi) \equiv \frac{4a^2}{[(a^2 - 1) \cos \theta + (a^2 + 1)]^2} .$$

Wavelet analysis formula

- **Wavelets on the sphere** may now be constructed from rotations and dilations of a mother spherical wavelet $\Phi \in L^2(S^2, d\Omega(\omega))$. The corresponding wavelet family $\{\Phi_{a,\rho} \equiv \mathcal{R}(\rho)\mathcal{D}(a)\Phi : \rho \in \text{SO}(3), a \in \mathbb{R}_*^+\}$ provides an over-complete set of functions in $L^2(S^2, d\Omega(\omega))$.
- The **CSWT** of $f \in L^2(S^2, d\Omega(\omega))$ is given by the projection on to each wavelet atom in the usual manner:

$$\widehat{\mathcal{W}}_{\Phi}^f(a, \rho) = \langle f, \Phi_{a,\rho} \rangle = \int_{S^2} d\Omega(\omega) f(\omega) \Phi_{a,\rho}^*(\omega),$$

where $d\Omega(\omega) = \sin \theta d\theta d\varphi$ is the usual invariant measure on the sphere.

- Transform general in the sense that all orientations in the rotation group $\text{SO}(3)$ are considered, thus **directional structure is naturally incorporated**.
- **Fast algorithms essential** (for a review see Wiaux *et al.* 2007)
 - Factoring of rotations: JDM *et al.* 2007
 - Separation of variables: Wiaux *et al.* 2005

Wavelet analysis formula

- **Wavelets on the sphere** may now be constructed from rotations and dilations of a mother spherical wavelet $\Phi \in L^2(S^2, d\Omega(\omega))$. The corresponding wavelet family $\{\Phi_{a,\rho} \equiv \mathcal{R}(\rho)\mathcal{D}(a)\Phi : \rho \in \text{SO}(3), a \in \mathbb{R}_*^+\}$ provides an over-complete set of functions in $L^2(S^2, d\Omega(\omega))$.
- The **CSWT** of $f \in L^2(S^2, d\Omega(\omega))$ is given by the projection on to each wavelet atom in the usual manner:

$$\widehat{\mathcal{W}}_{\Phi}^f(a, \rho) = \langle f, \Phi_{a,\rho} \rangle = \int_{S^2} d\Omega(\omega) f(\omega) \Phi_{a,\rho}^*(\omega),$$

where $d\Omega(\omega) = \sin \theta d\theta d\varphi$ is the usual invariant measure on the sphere.

- Transform general in the sense that all orientations in the rotation group $\text{SO}(3)$ are considered, thus **directional structure is naturally incorporated**.
- **Fast algorithms essential** (for a review see Wiaux *et al.* 2007)
 - Factoring of rotations: JDM *et al.* 2007
 - Separation of variables: Wiaux *et al.* 2005

Wavelet analysis formula

- **Wavelets on the sphere** may now be constructed from rotations and dilations of a mother spherical wavelet $\Phi \in L^2(S^2, d\Omega(\omega))$. The corresponding wavelet family $\{\Phi_{a,\rho} \equiv \mathcal{R}(\rho)\mathcal{D}(a)\Phi : \rho \in \text{SO}(3), a \in \mathbb{R}_*^+\}$ provides an over-complete set of functions in $L^2(S^2, d\Omega(\omega))$.
- The **CSWT** of $f \in L^2(S^2, d\Omega(\omega))$ is given by the projection on to each wavelet atom in the usual manner:

$$\widehat{W}_\Phi^f(a, \rho) = \langle f, \Phi_{a,\rho} \rangle = \int_{S^2} d\Omega(\omega) f(\omega) \Phi_{a,\rho}^*(\omega),$$

where $d\Omega(\omega) = \sin \theta d\theta d\varphi$ is the usual invariant measure on the sphere.

- Transform general in the sense that all orientations in the rotation group $\text{SO}(3)$ are considered, thus **directional structure is naturally incorporated**.
- **Fast algorithms essential** (for a review see Wiaux *et al.* 2007)
 - Factoring of rotations: JDM *et al.* 2007
 - Separation of variables: Wiaux *et al.* 2005

Wavelet synthesis formula

- The **synthesis** of a signal on the sphere from its wavelet coefficients is given by

$$f(\omega) = \int_0^\infty \frac{da}{a^3} \int_{\text{SO}(3)} d\rho(\rho) \widehat{\mathcal{W}}_\Phi^f(a, \rho) [\mathcal{R}(\rho) \widehat{L}_\Phi \Phi_a](\omega),$$

where $d\rho(\rho) = \sin \beta d\alpha d\beta d\gamma$ is the invariant measure on the rotation group $\text{SO}(3)$.

- The \widehat{L}_Φ operator in $L^2(\mathbb{S}^2, d\Omega(\omega))$ is defined by the action

$$(\widehat{L}_\Phi g)_{\ell m} \equiv g_{\ell m} / \widehat{C}_\Phi^\ell$$

on the spherical harmonic coefficients of functions $g \in L^2(\mathbb{S}^2, d\Omega(\omega))$.

- In order to ensure the perfect reconstruction of a signal synthesised from its wavelet coefficients, the **admissibility condition**

$$0 < \widehat{C}_\Phi^\ell \equiv \frac{8\pi^2}{2\ell + 1} \sum_{m=-\ell}^{\ell} \int_0^\infty \frac{da}{a^3} |(\Phi_a)_{\ell m}|^2 < \infty$$

must be satisfied for all $\ell \in \mathbb{N}$, where $(\Phi_a)_{\ell m}$ are the spherical harmonic coefficients of $\Phi_a(\omega)$.

Wavelet synthesis formula

- The **synthesis** of a signal on the sphere from its wavelet coefficients is given by

$$f(\omega) = \int_0^\infty \frac{da}{a^3} \int_{\text{SO}(3)} d\rho(\rho) \widehat{\mathcal{W}}_\Phi^f(a, \rho) [\mathcal{R}(\rho) \widehat{L}_\Phi \Phi_a](\omega),$$

where $d\rho(\rho) = \sin \beta d\alpha d\beta d\gamma$ is the invariant measure on the rotation group $\text{SO}(3)$.

- The \widehat{L}_Φ operator in $L^2(\mathbb{S}^2, d\Omega(\omega))$ is defined by the action

$$(\widehat{L}_\Phi g)_{\ell m} \equiv g_{\ell m} / \widehat{C}_\Phi^\ell$$

on the spherical harmonic coefficients of functions $g \in L^2(\mathbb{S}^2, d\Omega(\omega))$.

- In order to ensure the perfect reconstruction of a signal synthesised from its wavelet coefficients, the **admissibility condition**

$$0 < \widehat{C}_\Phi^\ell \equiv \frac{8\pi^2}{2\ell + 1} \sum_{m=-\ell}^{\ell} \int_0^\infty \frac{da}{a^3} |(\Phi_a)_{\ell m}|^2 < \infty$$

must be satisfied for all $\ell \in \mathbb{N}$, where $(\Phi_a)_{\ell m}$ are the spherical harmonic coefficients of $\Phi_a(\omega)$.

Correspondence principle

- **Correspondence principle** between spherical and Euclidean wavelets states that the inverse stereographic projection of an *admissible* wavelet on the plane yields an *admissible* wavelet on the sphere (proved by Wiaux *et al.* 2005)
- **Mother wavelets on sphere** constructed from the projection of mother Euclidean wavelets defined on the plane:

$$\Phi = \Pi^{-1} \Phi_{\mathbb{R}^2},$$

where $\Phi_{\mathbb{R}^2} \in L^2(\mathbb{R}^2, d^2\mathbf{x})$ is an admissible wavelet in the plane.

- **Directional wavelets on sphere** may be naturally constructed in this setting – they are simply the projection of directional Euclidean planar wavelets on to the sphere.

Correspondence principle

- **Correspondence principle** between spherical and Euclidean wavelets states that the inverse stereographic projection of an *admissible* wavelet on the plane yields an *admissible* wavelet on the sphere (proved by Wiaux *et al.* 2005)
- **Mother wavelets on sphere** constructed from the projection of mother Euclidean wavelets defined on the plane:

$$\Phi = \Pi^{-1} \Phi_{\mathbb{R}^2},$$

where $\Phi_{\mathbb{R}^2} \in L^2(\mathbb{R}^2, d^2\mathbf{x})$ is an admissible wavelet in the plane.

- **Directional wavelets on sphere** may be naturally constructed in this setting – they are simply the projection of directional Euclidean planar wavelets on to the sphere.

Correspondence principle

- **Correspondence principle** between spherical and Euclidean wavelets states that the inverse stereographic projection of an *admissible* wavelet on the plane yields an *admissible* wavelet on the sphere (proved by Wiaux *et al.* 2005)
- **Mother wavelets on sphere** constructed from the projection of mother Euclidean wavelets defined on the plane:

$$\Phi = \Pi^{-1} \Phi_{\mathbb{R}^2},$$

where $\Phi_{\mathbb{R}^2} \in L^2(\mathbb{R}^2, d^2x)$ is an admissible wavelet in the plane.

- **Directional wavelets on sphere** may be naturally constructed in this setting – they are simply the projection of directional Euclidean planar wavelets on to the sphere.

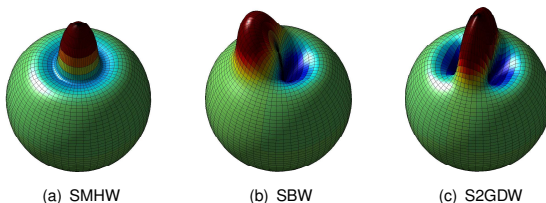


Figure: Spherical wavelets at scale $a, b = 0.2$.

Multiresolution analysis on the sphere

- Define multiresolution analysis on the sphere in an analogous manner to Euclidean framework.
- Define **approximation spaces** on the sphere $V_j \subset L^2(S^2)$
- Construct the **nested hierarchy** of approximation spaces

$$V_1 \subset V_2 \subset \cdots \subset V_j \subset L^2(S^2),$$

where coarser (finer) approximation spaces correspond to a lower (higher) resolution level j .

- For each space V_j we define a basis with basis elements given by the **scaling functions** $\varphi_{j,k} \in V_j$, where the k index corresponds to a translation on the sphere.
- Define **detail space** W_j to be the orthogonal complement of V_j in V_{j+1} , i.e. $V_{j+1} = V_j \oplus W_j$.
- For each space W_j we define a basis with basis elements given by the **wavelets** $\psi_{j,k} \in W_j$.
- Expanding the hierarchy of approximation spaces:

$$V_j = V_1 \oplus \bigoplus_{j=1}^{j-1} W_j.$$

Multiresolution analysis on the sphere

- Define multiresolution analysis on the sphere in an analogous manner to Euclidean framework.
- Define **approximation spaces** on the sphere $V_j \subset L^2(S^2)$
- Construct the **nested hierarchy** of approximation spaces

$$V_1 \subset V_2 \subset \cdots \subset V_j \subset L^2(S^2),$$

where coarser (finer) approximation spaces correspond to a lower (higher) resolution level j .

- For each space V_j we define a basis with basis elements given by the **scaling functions** $\varphi_{j,k} \in V_j$, where the k index corresponds to a translation on the sphere.
- Define **detail space** W_j to be the orthogonal complement of V_j in V_{j+1} , i.e. $V_{j+1} = V_j \oplus W_j$.
- For each space W_j we define a basis with basis elements given by the **wavelets** $\psi_{j,k} \in W_j$.
- Expanding the hierarchy of approximation spaces:

$$V_j = V_1 \oplus \bigoplus_{j=1}^{j-1} W_j.$$

Multiresolution analysis on the sphere

- Define multiresolution analysis on the sphere in an analogous manner to Euclidean framework.
- Define **approximation spaces** on the sphere $V_j \subset L^2(S^2)$
- Construct the **nested hierarchy** of approximation spaces

$$V_1 \subset V_2 \subset \cdots \subset V_J \subset L^2(S^2),$$

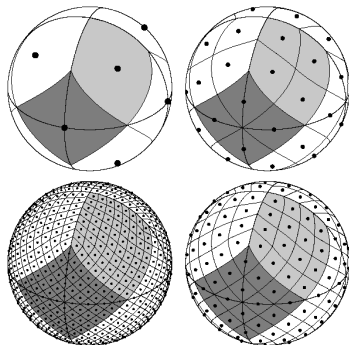
where coarser (finer) approximation spaces correspond to a lower (higher) resolution level j .

- For each space V_j we define a basis with basis elements given by the **scaling functions** $\varphi_{j,k} \in V_j$, where the k index corresponds to a translation on the sphere.
- Define **detail space** W_j to be the orthogonal complement of V_j in V_{j+1} , i.e. $V_{j+1} = V_j \oplus W_j$.
- For each space W_j we define a basis with basis elements given by the **wavelets** $\psi_{j,k} \in W_j$.
- Expanding the hierarchy of approximation spaces:

$$V_J = V_1 \oplus \bigoplus_{j=1}^{J-1} W_j.$$

Hierarchical pixelisation of the sphere

- Relate generic multiresolution decomposition to **HEALPix** hierarchical pixelisation of the sphere.



Credit: Krzysztof Gorski

Haar wavelets on the sphere

- Let V_j correspond to a HEALPix pixelised sphere with resolution parameter $N_{\text{side}} = 2^{j-1}$.
- Define the **scaling function** $\varphi_{j,k}$ at level j to be constant for pixel k and zero elsewhere:

$$\varphi_{j,k}(\omega) \equiv \begin{cases} 1/\sqrt{A_j} & \omega \in P_{j,k} \\ 0 & \text{elsewhere} . \end{cases}$$

- Orthonormal basis for the wavelet space W_j given by the following **wavelets**:

$$\psi_{j,k}^0(\omega) \equiv [\varphi_{j+1,k_0}(\omega) - \varphi_{j+1,k_1}(\omega) + \varphi_{j+1,k_2}(\omega) - \varphi_{j+1,k_3}(\omega)]/2 ;$$

$$\psi_{j,k}^1(\omega) \equiv [\varphi_{j+1,k_0}(\omega) + \varphi_{j+1,k_1}(\omega) - \varphi_{j+1,k_2}(\omega) - \varphi_{j+1,k_3}(\omega)]/2 ;$$

$$\psi_{j,k}^2(\omega) \equiv [\varphi_{j+1,k_0}(\omega) - \varphi_{j+1,k_1}(\omega) - \varphi_{j+1,k_2}(\omega) + \varphi_{j+1,k_3}(\omega)]/2 .$$

Haar wavelets on the sphere

- Let V_j correspond to a HEALPix pixelised sphere with resolution parameter $N_{\text{side}} = 2^{j-1}$.
- Define the **scaling function** $\varphi_{j,k}$ at level j to be constant for pixel k and zero elsewhere:

$$\varphi_{j,k}(\omega) \equiv \begin{cases} 1/\sqrt{A_j} & \omega \in P_{j,k} \\ 0 & \text{elsewhere} . \end{cases}$$

- Orthonormal basis for the wavelet space W_j given by the following **wavelets**:

$$\psi_{j,k}^0(\omega) \equiv [\varphi_{j+1,k_0}(\omega) - \varphi_{j+1,k_1}(\omega) + \varphi_{j+1,k_2}(\omega) - \varphi_{j+1,k_3}(\omega)]/2 ;$$

$$\psi_{j,k}^1(\omega) \equiv [\varphi_{j+1,k_0}(\omega) + \varphi_{j+1,k_1}(\omega) - \varphi_{j+1,k_2}(\omega) - \varphi_{j+1,k_3}(\omega)]/2 ;$$

$$\psi_{j,k}^2(\omega) \equiv [\varphi_{j+1,k_0}(\omega) - \varphi_{j+1,k_1}(\omega) - \varphi_{j+1,k_2}(\omega) + \varphi_{j+1,k_3}(\omega)]/2 .$$

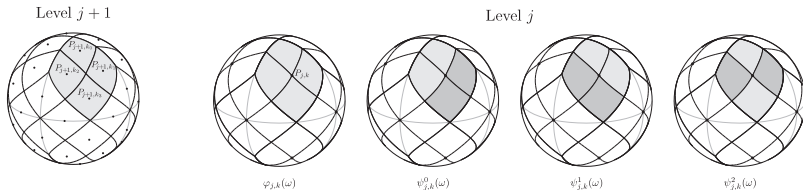


Figure: Haar scaling function $\varphi_{j,k}(\omega)$ and wavelets $\psi_{j,k}^m(\omega)$

Haar wavelets on the sphere

- **Multiresolution decomposition** of a function defined on a HEALPix data-sphere at resolution J , i.e. $f_J \in V_J$ proceeds as follows.
- **Approximation** coefficients at the coarser level j are given by the projection of f_{j+1} onto the scaling functions $\varphi_{j,k}$:

$$\lambda_{j,k} = \int_{S^2} f_{j+1}(\omega) \varphi_{j,k}(\omega) \, d\Omega .$$

- **Detail coefficients** at level j are given by the projection of f_{j+1} onto the wavelets $\psi_{j,k}^m$:

$$\gamma_{j,k}^m = \int_{S^2} f_{j+1}(\omega) \psi_{j,k}^m(\omega) \, d\Omega .$$

- The function $f_J \in V_J$ may then be **synthesised** from its approximation and detail coefficients:

$$f_J(\omega) = \sum_{k=0}^{N_{J_0}-1} \lambda_{J_0,k} \varphi_{J_0,k}(\omega) + \sum_{j=J_0}^{J-1} \sum_{k=0}^{N_j-1} \sum_{m=0}^2 \gamma_{j,k}^m \psi_{j,k}^m(\omega) .$$

Haar wavelets on the sphere

- **Multiresolution decomposition** of a function defined on a HEALPix data-sphere at resolution J , i.e. $f_J \in V_J$ proceeds as follows.
- **Approximation** coefficients at the coarser level j are given by the projection of f_{j+1} onto the scaling functions $\varphi_{j,k}$:

$$\lambda_{j,k} = \int_{S^2} f_{j+1}(\omega) \varphi_{j,k}(\omega) d\Omega .$$

- **Detail coefficients** at level j are given by the projection of f_{j+1} onto the wavelets $\psi_{j,k}^m$:

$$\gamma_{j,k}^m = \int_{S^2} f_{j+1}(\omega) \psi_{j,k}^m(\omega) d\Omega .$$

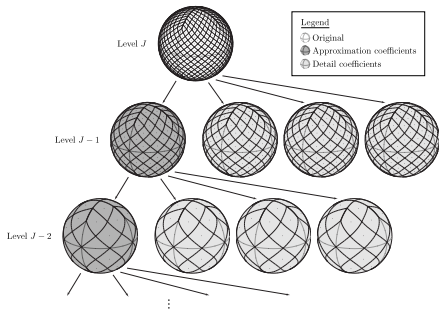


Figure: Haar multiresolution decomposition

- The function $f_j \in V_j$ may then be **synthesised** from its approximation and detail coefficients:

$$f_j(\omega) = \sum_{k=0}^{N_{j_0}-1} \lambda_{j_0,k} \varphi_{j_0,k}(\omega) + \sum_{j=j_0}^{j-1} \sum_{k=0}^{N_j-1} \sum_{m=0}^2 \gamma_{j,k}^m \psi_{j,k}^m(\omega) .$$

Haar wavelets on the sphere

- **Multiresolution decomposition** of a function defined on a HEALPix data-sphere at resolution J , i.e. $f_J \in V_J$ proceeds as follows.
- **Approximation** coefficients at the coarser level j are given by the projection of f_{j+1} onto the scaling functions $\varphi_{j,k}$:

$$\lambda_{j,k} = \int_{S^2} f_{j+1}(\omega) \varphi_{j,k}(\omega) d\Omega .$$

- **Detail coefficients** at level j are given by the projection of f_{j+1} onto the wavelets $\psi_{j,k}^m$:

$$\gamma_{j,k}^m = \int_{S^2} f_{j+1}(\omega) \psi_{j,k}^m(\omega) d\Omega .$$

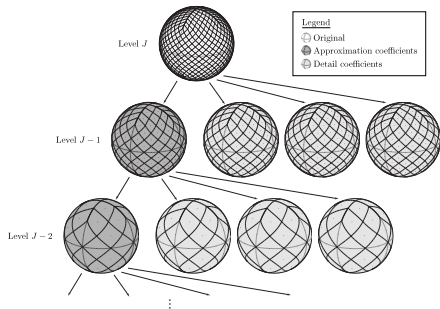


Figure: Haar multiresolution decomposition

- The function $f_j \in V_j$ may then be **synthesised** from its approximation and detail coefficients:

$$f_j(\omega) = \sum_{k=0}^{N_{J_0}-1} \lambda_{J_0,k} \varphi_{J_0,k}(\omega) + \sum_{j=J_0}^{J-1} \sum_{k=0}^{N_j-1} \sum_{m=0}^2 \gamma_{j,k}^m \psi_{j,k}^m(\omega) .$$

Outline

- 1 Cosmology
 - Big Bang
 - Cosmic microwave background
 - Observations
- 2 Harmonic analysis on the sphere
 - Spherical harmonic transform
 - Sampling theorems
- 3 Wavelets on the sphere
 - Why wavelets?
 - Continuous wavelets
 - Multiresolution analysis
- 4 Applications
 - Gaussianity of the CMB
 - Dark energy
 - Compression
 - Reflectance recovery

Gaussianity of the CMB

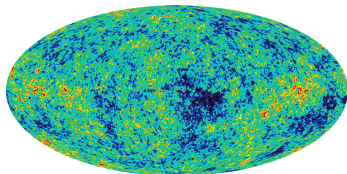
- **Statistics of primordial fluctuations** provide a useful mechanism for distinguishing between various scenarios of the early Universe, such as various models of inflation.
- Primordial fluctuations give rise to the CMB anisotropies.
- In the simplest inflationary scenarios, primordial perturbations seed Gaussian temperature fluctuations in the CMB.
- However, this is not the case for non-standard inflationary models.
- **Evidence of non-Gaussianity in the CMB anisotropies would therefore have profound implications for the standard cosmological concordance model.**
- Probe WMAP observations of the CMB for evidence of non-Gaussianity.

Gaussianity of the CMB

- **Statistics of primordial fluctuations** provide a useful mechanism for distinguishing between various scenarios of the early Universe, such as various models of inflation.
- Primordial fluctuations give rise to the CMB anisotropies.
- In the simplest inflationary scenarios, primordial perturbations seed Gaussian temperature fluctuations in the CMB.
- However, this is not the case for non-standard inflationary models.
- **Evidence of non-Gaussianity in the CMB anisotropies would therefore have profound implications for the standard cosmological concordance model.**
- Probe WMAP observations of the CMB for evidence of non-Gaussianity.

Gaussianity of the CMB

- **Statistics of primordial fluctuations** provide a useful mechanism for distinguishing between various scenarios of the early Universe, such as various models of inflation.
- Primordial fluctuations give rise to the CMB anisotropies.
- In the simplest inflationary scenarios, primordial perturbations seed Gaussian temperature fluctuations in the CMB.
- However, this is not the case for non-standard inflationary models.
- **Evidence of non-Gaussianity in the CMB anisotropies would therefore have profound implications for the standard cosmological concordance model.**
- Probe WMAP observations of the CMB for evidence of non-Gaussianity.



Wavelet analysis of Gaussianity of the CMB

- Various physical processes manifest at different scales and locations, hence employ wavelet analysis to probe CMB.
- Wavelet coefficients of Gaussian signal remain Gaussian distributed (due to linearity of wavelet transform).
- Examine the skewness and kurtosis of wavelet coefficients.
- Compare to Monte Carlo simulations of Gaussian CMB realisations.
- Significant non-Gaussian signal detected in the skewness of wavelet coefficients.

Wavelet analysis of Gaussianity of the CMB

- Various physical processes manifest at different scales and locations, hence employ wavelet analysis to probe CMB.
- Wavelet coefficients of Gaussian signal remain Gaussian distributed (due to linearity of wavelet transform).
- Examine the skewness and kurtosis of wavelet coefficients.
- Compare to Monte Carlo simulations of Gaussian CMB realisations.
- **Significant non-Gaussian signal detected** in the skewness of wavelet coefficients.

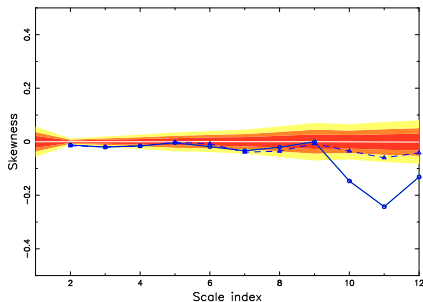


Figure: Skewness of wavelet coefficients

Wavelet analysis of Gaussianity of the CMB

- Various physical processes manifest at different scales and locations, hence employ wavelet analysis to probe CMB.
- Wavelet coefficients of Gaussian signal remain Gaussian distributed (due to linearity of wavelet transform).
- Examine the skewness and kurtosis of wavelet coefficients.
- Compare to Monte Carlo simulations of Gaussian CMB realisations.
- **Significant non-Gaussian signal detected** in the skewness of wavelet coefficients.

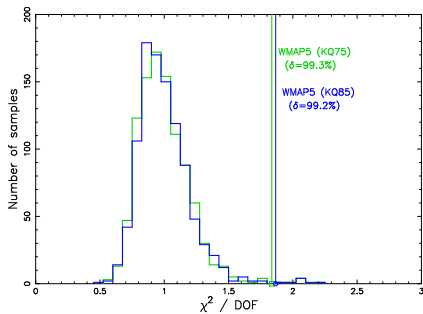


Figure: χ^2 of skewness of wavelet coefficients

Localisation of non-Gaussian features in the CMB

- Localise regions that contribute most significantly to the non-Gaussian signal.
- Detection of the "cold spot" anomaly in the CMB.
- Various new cosmology models constructed in attempt to explain the cold spot.

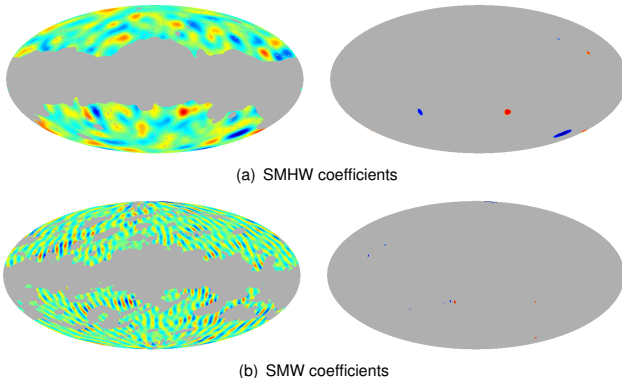


Figure: Spherical wavelet coefficient maps (left) and thresholded maps (right)

Localisation of non-Gaussian features in the CMB

- Localise regions that contribute most significantly to the non-Gaussian signal.
- Detection of the “cold spot” anomaly in the CMB.
- Various **new cosmology models** constructed in attempt to explain the cold spot.

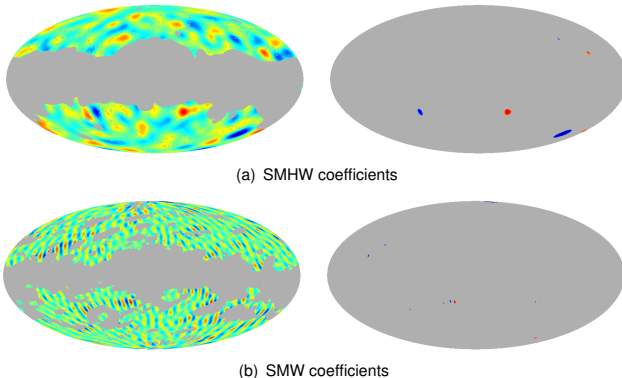
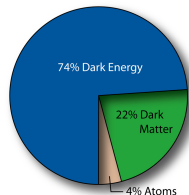


Figure: Spherical wavelet coefficient maps (left) and thresholded maps (right)

Dark energy

- Universe consists of ordinary baryonic matter, cold dark matter and dark energy.
- **Dark energy represents energy density of empty space.** Modelled by a cosmological fluid with negative pressure acting as a repulsive force.
- Evidence for dark energy provided by observations of CMB, supernovae and large scale structure of Universe.

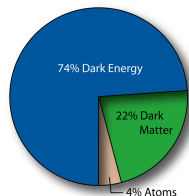


Credit: WMAP Science Team

- However, a **consistent model in the framework of particle physics lacking**. Indeed, attempts to predict a cosmological constant obtain a value that is too large by a factor of $\sim 10^{120}$.
- Dark energy dominates our Universe but yet **we know very little about its nature and origin**.
- Verification of dark energy by **independent physical methods** of considerable interest.
- Independent methods may also prove more sensitive **probes of properties of dark energy**.

Dark energy

- Universe consists of ordinary baryonic matter, cold dark matter and dark energy.
- **Dark energy represents energy density of empty space.** Modelled by a cosmological fluid with negative pressure acting as a repulsive force.
- Evidence for dark energy provided by observations of CMB, supernovae and large scale structure of Universe.

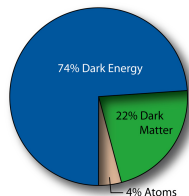


Credit: WMAP Science Team

- However, a **consistent model in the framework of particle physics lacking**. Indeed, attempts to predict a cosmological constant obtain a value that is too large by a factor of $\sim 10^{120}$.
- Dark energy dominates our Universe but yet **we know very little about its nature and origin**.
- Verification of dark energy by **independent physical methods** of considerable interest.
- Independent methods may also prove more sensitive **probes of properties of dark energy**.

Dark energy

- Universe consists of ordinary baryonic matter, cold dark matter and dark energy.
- **Dark energy represents energy density of empty space.** Modelled by a cosmological fluid with negative pressure acting as a repulsive force.
- Evidence for dark energy provided by observations of CMB, supernovae and large scale structure of Universe.



Credit: WMAP Science Team

- However, a **consistent model in the framework of particle physics lacking.** Indeed, attempts to predict a cosmological constant obtain a value that is too large by a factor of $\sim 10^{120}$.
- Dark energy dominates our Universe but yet **we know very little about its nature and origin.**
- Verification of dark energy by **independent physical methods** of considerable interest.
- Independent methods may also prove more sensitive **probes of properties of dark energy.**

Integrated Sachs-Wolfe (ISW) effect

(ball sim constant movie)

(ball sim evolving movie)

Figure: ISW effect analogy

- CMB photons blue (red) shifted when fall into (out of) potential wells.
- **Evolution of potential** during photon propagation → **net change in photon energy**.
- Gravitation potentials constant w.r.t. conformal time in matter dominated universe.
- Deviation from matter domination due to curvature or **dark energy** causes **potentials to evolve** with time → **secondary anisotropy** induced in CMB.

Detecting the ISW effect

- WMAP shown universe is (nearly) flat.
- Detection of ISW effect \Rightarrow direct **evidence for dark energy**.
- Cannot isolate the ISW signal from CMB anisotropies easily.
- Instead, **detect by cross-correlating** CMB anisotropies with tracers of large scale structure. (Crittenden & Turok 1996)
- Wavelets **ideal analysis tool** to search for correlation induced by ISW effect since signal manifest at different scales and locations. (Pioneered by Vielva *et al.* 2005, followed by JDM *et al.* 2006, JDM *et al.* 2007 and others.)
- Compute correlation of WMAP and NVSS radio galaxy survey and compare to Monte Carlo simulations to determine significance of any candidate detections.

Detecting the ISW effect

- WMAP shown universe is (nearly) flat.
- Detection of ISW effect \Rightarrow direct **evidence for dark energy**.
- Cannot isolate the ISW signal from CMB anisotropies easily.
- Instead, **detect by cross-correlating** CMB anisotropies with tracers of large scale structure. (Crittenden & Turok 1996)
- Wavelets **ideal analysis tool** to search for correlation induced by ISW effect since signal manifest at different scales and locations. (Pioneered by Vielva *et al.* 2005, followed by JDM *et al.* 2006, JDM *et al.* 2007 and others.)
- Compute correlation of WMAP and NVSS radio galaxy survey and compare to Monte Carlo simulations to determine significance of any candidate detections.

Detecting the ISW effect

- WMAP shown universe is (nearly) flat.
- Detection of ISW effect \Rightarrow direct **evidence for dark energy**.
- Cannot isolate the ISW signal from CMB anisotropies easily.
- Instead, **detect by cross-correlating** CMB anisotropies with tracers of large scale structure. (Crittenden & Turok 1996)
- Wavelets **ideal analysis tool** to search for correlation induced by ISW effect since signal manifest at different scales and locations. (Pioneered by Vielva *et al.* 2005, followed by JDM *et al.* 2006, JDM *et al.* 2007 and others.)
- Compute correlation of WMAP and NVSS radio galaxy survey and compare to Monte Carlo simulations to determine significance of any candidate detections.

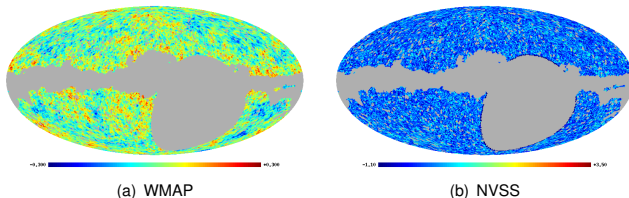


Figure: WMAP and NVSS maps after application of the joint mask

Detection of the ISW effect with wavelets

- **Significant correlation detected** between the WMAP and NVSS data.
- Foreground contamination and instrumental systematics ruled out as source of the correlation
⇒ correlation due to ISW effect.
- **Direct observational evidence for dark energy.**

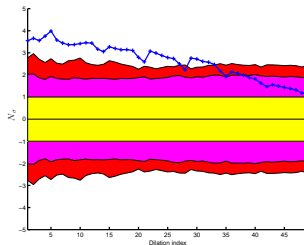


Figure: Wavelet correlation

Detection of the ISW effect with wavelets

- **Significant correlation detected** between the WMAP and NVSS data.
- Foreground contamination and instrumental systematics ruled out as source of the correlation
⇒ correlation due to ISW effect.
- **Direct observational evidence for dark energy.**

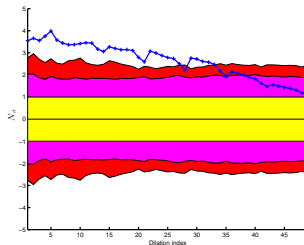


Figure: Wavelet correlation

Constraining dark energy with wavelets

- Possible to use positive detection of the ISW effect to **constrain parameters** of cosmological models **that describe dark energy**:
 - Proportional energy density Ω_Λ .
 - Equation of state parameter w relating pressure and density of cosmological fluid that models dark energy, *i.e.* $p = w\rho$.
- **Parameter estimates** of $\Omega_\Lambda = 0.63^{+0.18}_{-0.17}$ and $w = -0.77^{+0.35}_{-0.36}$ computed from the mean of the marginalised distributions (consistent with other analysis techniques and data sets).

Constraining dark energy with wavelets

- Possible to use positive detection of the ISW effect to **constrain parameters** of cosmological models **that describe dark energy**:
 - Proportional energy density Ω_Λ .
 - Equation of state parameter w relating pressure and density of cosmological fluid that models dark energy, *i.e.* $p = w\rho$.
- **Parameter estimates** of $\Omega_\Lambda = 0.63^{+0.18}_{-0.17}$ and $w = -0.77^{+0.35}_{-0.36}$ computed from the mean of the marginalised distributions (consistent with other analysis techniques and data sets).

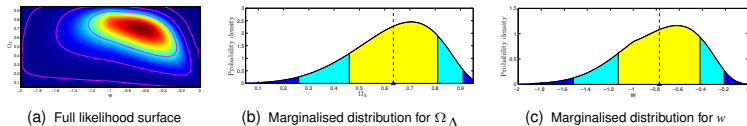
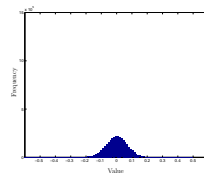


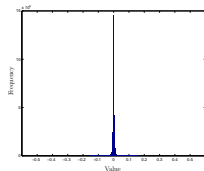
Figure: Dark energy likelihoods

Compression of data on the sphere

- Current and forthcoming observations of the CMB of considerable size.
- Haar wavelet transform to **compress energy content**.



(a) Original data



(b) Wavelet coefficients

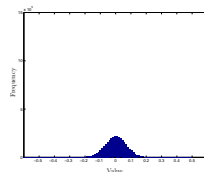
Figure: Histograms

Compression of data on the sphere

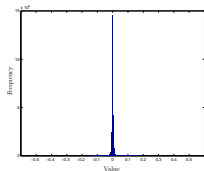
- Current and forthcoming observations of the CMB of considerable size.
- Haar wavelet transform to **compress energy content**.

Lossless compression algorithm

- 1 Haar wavelet transform on sphere
- 2 Quantise detail coefficients to numerical precision (precision parameter p)
- 3 Huffman encoding



(a) Original data



(b) Wavelet coefficients

Figure: Histograms

Compression of data on the sphere

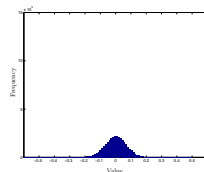
- Current and forthcoming observations of the CMB of considerable size.
- Haar wavelet transform to **compress energy content**.

Lossless compression algorithm

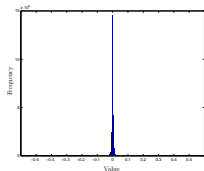
- 1 Haar wavelet transform on sphere
- 2 Quantise detail coefficients to numerical precision (precision parameter p)
- 3 Huffman encoding

Lossy compression algorithm

- 1 Haar wavelet transform on sphere
- 2 Thresholding
- 3 Quantise detail coefficients to numerical precision
- 4 Run-length encoding (RLE)
- 5 Huffman encoding



(a) Original data



(b) Wavelet coefficients

Figure: Histograms

Compression of CMB data

- Lossless to a user specified numerical precision only.

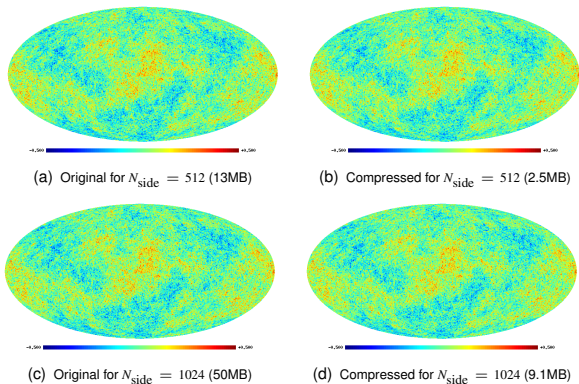
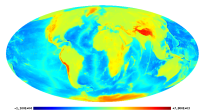
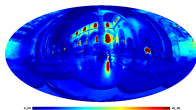


Figure: Lossless compression of simulated Gaussian CMB data

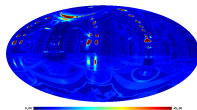
Lossy compression applications



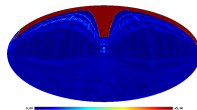
(a) Earth: original (13MB)



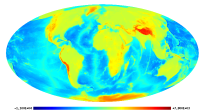
(b) Galileo: original (3.2MB)



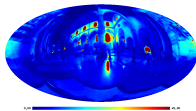
(c) St Peter's: original (3.2MB)



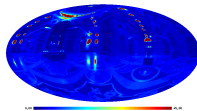
(d) Uffizi: original (3.2MB)



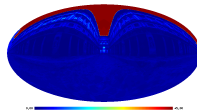
(e) Earth: lossless (1.4MB)



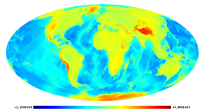
(f) Galileo: lossless (0.21MB)



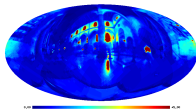
(g) St Peter's: lossless (0.20MB)



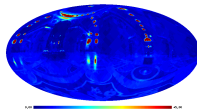
(h) Uffizi: lossless (0.19MB)



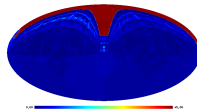
(i) Earth: lossy (0.33MB)



(j) Galileo: lossy (0.07MB)



(k) St Peter's: lossy (0.08MB)



(l) Uffizi: lossy (0.10MB)

Figure: Compressed data for lossy compression applications

Reflectance recovery

- Functions encountered in **computer graphics** are typically defined over directions → data on the sphere.
- **Illumination maps** inherently defined on the sphere (*i.e.* over directions):

Let $L(\omega)$ denote the illumination function, where $\omega = (\theta, \varphi) \in S^2$.

- Bidirectional reflectance distributions functions (**BRDFs**) inherently defined on the product of spheres:

Let $\bar{\Gamma}(\omega_i, \omega_o)$ denote the BRDF, where ω_i and ω_o are incoming and outgoing directions respectively.

Reflectance recovery

- Functions encountered in **computer graphics** are typically defined over directions
→ data on the sphere.
- **Illumination maps** inherently defined on the sphere (*i.e.* over directions):

Let $L(\omega)$ denote the illumination function, where $\omega = (\theta, \varphi) \in S^2$.

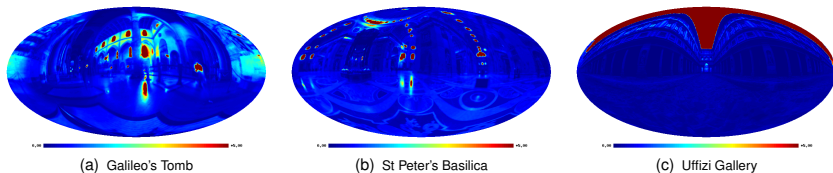


Figure: Illumination maps [<http://www.debevec.org/Probes>]

- Bidirectional reflectance distributions functions (**BRDFs**) inherently defined on the product of spheres:

Let $\tilde{F}(\omega_i, \omega_o)$ denote the BRDF, where ω_i and ω_o are incoming and outgoing directions respectively.

Theoretical framework for reflection

- Adopt the framework of **Ramamoorthi & Hanrahan (2001)**.
- Outgoing radiance given by

$$B(\rho, \omega_0) = \int_{S^2} L(\omega'_i) \bar{\Gamma}(\omega_i, \omega_0) \cos(\theta_i) \, d\Omega(\omega_i) ,$$

where the prime denotes global coordinates, $\rho = (\alpha, \beta, \gamma) \in \text{SO}(3)$ is the orientation of the surface element (*cf.* surface normal) and $d\Omega(\omega) = \sin(\theta) \, d\theta \, d\varphi$ is the usual rotation invariant measure on the sphere.

- Local coordinates and global coordinates related through rotation \mathcal{R} about surface element $\omega' = \mathcal{R}(\rho) \omega$, hence in a consistent coordinate frame we obtain

$$B(\rho, \omega_0) = \int_{S^2} (\mathcal{R}^{-1}(\rho)L)(\omega_i) \Gamma(\omega_i, \omega_0) \, d\Omega(\omega_i) .$$

- Through the rotation invariance of the measure on the sphere we obtain the **reflection equation**

$$B(\rho, \omega_0) = \int_{S^2} L(\omega_i) (\mathcal{R}(\rho)\Gamma)(\omega_i, \omega_0) \, d\Omega(\omega_i) .$$

- Assumptions: homogenous object; known geometry; distant illumination; no inter-reflection.

Theoretical framework for reflection

- Adopt the framework of **Ramamoorthi & Hanrahan (2001)**.
- Outgoing radiance given by

$$B(\rho, \omega_0) = \int_{S^2} L(\omega'_i) \bar{\Gamma}(\omega_i, \omega_0) \cos(\theta_i) \, d\Omega(\omega_i) ,$$

where the prime denotes global coordinates, $\rho = (\alpha, \beta, \gamma) \in \text{SO}(3)$ is the orientation of the surface element (*cf.* surface normal) and $d\Omega(\omega) = \sin(\theta) \, d\theta \, d\varphi$ is the usual rotation invariant measure on the sphere.

- Local coordinates and global coordinates related through rotation \mathcal{R} about surface element $\omega' = \mathcal{R}(\rho) \omega$, hence in a consistent coordinate frame we obtain

$$B(\rho, \omega_0) = \int_{S^2} (\mathcal{R}^{-1}(\rho)L)(\omega_i) \Gamma(\omega_i, \omega_0) \, d\Omega(\omega_i) .$$

- Through the rotation invariance of the measure on the sphere we obtain the **reflection equation**

$$B(\rho, \omega_0) = \int_{S^2} L(\omega_i) (\mathcal{R}(\rho)\Gamma)(\omega_i, \omega_0) \, d\Omega(\omega_i) .$$

- Assumptions: homogenous object; known geometry; distant illumination; no inter-reflection.

Theoretical framework for reflection

- Adopt the framework of **Ramamoorthi & Hanrahan (2001)**.
- Outgoing radiance given by

$$B(\rho, \omega_0) = \int_{S^2} L(\omega'_i) \bar{\Gamma}(\omega_i, \omega_0) \cos(\theta_i) \, d\Omega(\omega_i) ,$$

where the prime denotes global coordinates, $\rho = (\alpha, \beta, \gamma) \in \text{SO}(3)$ is the orientation of the surface element (*cf.* surface normal) and $d\Omega(\omega) = \sin(\theta) \, d\theta \, d\varphi$ is the usual rotation invariant measure on the sphere.

- Local coordinates and global coordinates related through rotation \mathcal{R} about surface element $\omega' = \mathcal{R}(\rho) \omega$, hence in a consistent coordinate frame we obtain

$$B(\rho, \omega_0) = \int_{S^2} (\mathcal{R}^{-1}(\rho)L)(\omega_i) \Gamma(\omega_i, \omega_0) \, d\Omega(\omega_i) .$$

- Through the rotation invariance of the measure on the sphere we obtain the **reflection equation**

$$B(\rho, \omega_0) = \int_{S^2} L(\omega_i) (\mathcal{R}(\rho)\Gamma)(\omega_i, \omega_0) \, d\Omega(\omega_i) .$$

- Assumptions: homogenous object; known geometry; distant illumination; no inter-reflection.

Precomputed radiance transfer (PRT) using wavelets on the sphere

- Consider the **forward rendering** problem.

- Adopt the framework of **Ng *et al.* (2004)**.

Compute the outgoing radiance for each vertex of the object \mathbf{x} and incorporate a visibility function $V(\mathbf{x}, \omega_i)$. In this setting the reflection equation becomes

$$B(\mathbf{x}, \omega_o) = \int_{S^2} L(\omega_i) (\mathcal{R}(\rho(\mathbf{x}))\Gamma)(\omega_i, \omega_o) V(\mathbf{x}, \omega_i) d\Omega(\omega_i) .$$

- Very high computational complexity \rightarrow infeasible for practical purposes.

- Ng *et al.* resolve this issue by using **planar wavelets**.

- Adapted this approach to use **wavelets on the sphere** (Geomerics Ltd. 2006).

<http://www.geomerics.com>

Take geometry of the sphere into account \rightarrow greater accuracy and efficiency.

Precomputed radiance transfer (PRT) using wavelets on the sphere

- Consider the **forward rendering** problem.

- Adopt the framework of **Ng *et al.* (2004)**.

Compute the outgoing radiance for each vertex of the object \mathbf{x} and incorporate a visibility function $V(\mathbf{x}, \omega_i)$. In this setting the reflection equation becomes

$$B(\mathbf{x}, \omega_o) = \int_{S^2} L(\omega_i) (\mathcal{R}(\rho(\mathbf{x}))\Gamma)(\omega_i, \omega_o) V(\mathbf{x}, \omega_i) d\Omega(\omega_i) .$$

- Very high computational complexity \rightarrow infeasible for practical purposes.

- Ng *et al.* resolve this issue by using **planar wavelets**.

- Adapted this approach to use **wavelets on the sphere** (Geomerics Ltd. 2006).

<http://www.geomerics.com>

Take geometry of the sphere into account \rightarrow greater accuracy and efficiency.

Precomputed radiance transfer (PRT) using wavelets on the sphere

- Consider the **forward rendering** problem.

- Adopt the framework of **Ng *et al.* (2004)**.

Compute the outgoing radiance for each vertex of the object \mathbf{x} and incorporate a visibility function $V(\mathbf{x}, \omega_i)$. In this setting the reflection equation becomes

$$B(\mathbf{x}, \omega_o) = \int_{S^2} L(\omega_i) (\mathcal{R}(\rho(\mathbf{x}))\Gamma)(\omega_i, \omega_o) V(\mathbf{x}, \omega_i) d\Omega(\omega_i) .$$

- Very high computational complexity \rightarrow infeasible for practical purposes.

- Ng *et al.* resolve this issue by using **planar wavelets**.

- Adapted this approach to use **wavelets on the sphere** (Geomerics Ltd. 2006).

<http://www.geomerics.com>

Take geometry of the sphere into account \rightarrow greater accuracy and efficiency.

Reflectance recovery: current approaches

- Consider the **inverse rendering** problem, *i.e.* recover the BRDF from known outgoing radiance and known background illumination.
- Reflection equation again:

$$B(\rho, \omega_o) = \int_{S^2} L(\omega_i) (\mathcal{R}(\rho)\Gamma)(\omega_i, \omega_o) d\Omega(\omega_i)$$

- Many reflectance acquisition systems involve **specialised lighting configurations** which considerably simplify the inverse problem.

For example, point light source: $L(\omega_i) = \delta(\omega_i - \bar{\omega}) \Rightarrow B(\rho, \omega_o) = (\mathcal{R}(\rho)\Gamma)(\bar{\omega}, \omega_o)$.

- Disadvantages of current acquisition systems:
 - Slow
 - Specialised apparatus
 - Carefully controlled environment

→ **Painstaking and expensive process**

Reflectance recovery: current approaches

- Consider the **inverse rendering** problem, *i.e.* recover the BRDF from known outgoing radiance and known background illumination.
- Reflection equation again:

$$B(\rho, \omega_o) = \int_{S^2} L(\omega_i) (\mathcal{R}(\rho)\Gamma)(\omega_i, \omega_o) d\Omega(\omega_i)$$

- Many reflectance acquisition systems involve **specialised lighting configurations** which considerably simplify the inverse problem.

For example, point light source: $L(\omega_i) = \delta(\omega_i - \bar{\omega}) \Rightarrow B(\rho, \omega_o) = (\mathcal{R}(\rho)\Gamma)(\bar{\omega}, \omega_o)$.

- Disadvantages of current acquisition systems:
 - Slow
 - Specialised apparatus
 - Carefully controlled environment

→ **Painstaking and expensive process**

Reflectance recovery: current approaches

- Consider the **inverse rendering** problem, *i.e.* recover the BRDF from known outgoing radiance and known background illumination.
- Reflection equation again:

$$B(\rho, \omega_o) = \int_{S^2} L(\omega_i) (\mathcal{R}(\rho)\Gamma)(\omega_i, \omega_o) d\Omega(\omega_i)$$

- Many reflectance acquisition systems involve **specialised lighting configurations** which considerably simplify the inverse problem.

For example, point light source: $L(\omega_i) = \delta(\omega_i - \bar{\omega}) \Rightarrow B(\rho, \omega_o) = (\mathcal{R}(\rho)\Gamma)(\bar{\omega}, \omega_o)$.

- Disadvantages of current acquisition systems:
 - Slow
 - Specialised apparatus
 - Carefully controlled environment
 → **Painstaking and expensive process**

Reflectance recovery: proposed approach

- Reflection equation again:

$$B(\rho, \omega_0) = \int_{S^2} L(\omega_i) (\mathcal{R}(\rho)\Gamma)(\omega_i, \omega_0) d\Omega(\omega_i)$$

- **Solve the reflection equation directly**, under natural environmental illumination.
- Difficult inverse problem.
- **Shift the complexity** from elaborate experiment apparatus and procedures to more complicated algorithms but much simpler acquisition.
- Considered previously by Ramamoorthi & Hanrahan but limited to very low frequencies due to computational complexity → focused on **theoretical implications**.
- **Fast, spherical wavelet based methods.**
 - much higher frequencies computationally tractable
 - greater accuracy and performance
- Proposed acquisition system.
- Advantages of proposed acquisition system:
 - Fast acquisition
 - Standard apparatus
 - Acquisition performed in natural environment, *e.g.* on set/site (provided some conditions met)
 - **Flexible, fast and inexpensive process**

Reflectance recovery: proposed approach

- Reflection equation again:

$$B(\rho, \omega_0) = \int_{S^2} L(\omega_i) (\mathcal{R}(\rho)\Gamma)(\omega_i, \omega_0) d\Omega(\omega_i)$$

- **Solve the reflection equation directly**, under natural environmental illumination.
- Difficult inverse problem.
- **Shift the complexity** from elaborate experiment apparatus and procedures to more complicated algorithms but much simpler acquisition.
- Considered previously by Ramamoorthi & Hanrahan but limited to very low frequencies due to computational complexity → focused on **theoretical implications**.
- **Fast, spherical wavelet based methods**.
 - much higher frequencies computationally tractable
 - greater accuracy and performance
- Proposed acquisition system.
- Advantages of proposed acquisition system:
 - Fast acquisition
 - Standard apparatus
 - Acquisition performed in natural environment, *e.g.* on set/site (provided some conditions met)
 - **Flexible, fast and inexpensive process**

Reflectance recovery: proposed approach

- Reflection equation again:

$$B(\rho, \omega_0) = \int_{S^2} L(\omega_i) (\mathcal{R}(\rho)\Gamma)(\omega_i, \omega_0) d\Omega(\omega_i)$$

- **Solve the reflection equation directly**, under natural environmental illumination.
- Difficult inverse problem.
- **Shift the complexity** from elaborate experiment apparatus and procedures to more complicated algorithms but much simpler acquisition.
- Considered previously by Ramamoorthi & Hanrahan but limited to very low frequencies due to computational complexity → focused on **theoretical implications**.
- **Fast, spherical wavelet based methods.**
 - much higher frequencies computationally tractable
 - greater accuracy and performance
- Proposed acquisition system.
- Advantages of proposed acquisition system:
 - Fast acquisition
 - Standard apparatus
 - Acquisition performed in natural environment, *e.g.* on set/site (provided some conditions met)
 - **Flexible, fast and inexpensive process**

Reflectance recovery: proposed approach

- Reflection equation again:

$$B(\rho, \omega_0) = \int_{S^2} L(\omega_i) (\mathcal{R}(\rho)\Gamma)(\omega_i, \omega_0) d\Omega(\omega_i)$$

- **Solve the reflection equation directly**, under natural environmental illumination.
- Difficult inverse problem.
- **Shift the complexity** from elaborate experiment apparatus and procedures to more complicated algorithms but much simpler acquisition.
- Considered previously by Ramamoorthi & Hanrahan but limited to very low frequencies due to computational complexity → focused on **theoretical implications**.
- **Fast, spherical wavelet based methods.**
 - much higher frequencies computationally tractable
 - greater accuracy and performance
- Proposed acquisition system.
- Advantages of proposed acquisition system:
 - Fast acquisition
 - Standard apparatus
 - Acquisition performed in natural environment, *e.g.* on set/site (provided some conditions met)
 - **Flexible, fast and inexpensive process**

Reflectance recovery: proposed approach

- Reflection equation again:

$$B(\rho, \omega_0) = \int_{S^2} L(\omega_i) (\mathcal{R}(\rho)\Gamma)(\omega_i, \omega_0) d\Omega(\omega_i)$$

- **Solve the reflection equation directly**, under natural environmental illumination.
- Difficult inverse problem.
- **Shift the complexity** from elaborate experiment apparatus and procedures to more complicated algorithms but much simpler acquisition.
- Considered previously by Ramamoorthi & Hanrahan but limited to very low frequencies due to computational complexity → focused on **theoretical implications**.
- **Fast, spherical wavelet based methods**.
 - much higher frequencies computationally tractable
 - greater accuracy and performance
- Proposed acquisition system.
- Advantages of proposed acquisition system:
 - Fast acquisition
 - Standard apparatus
 - Acquisition performed in natural environment, *e.g.* on set/site (provided some conditions met)
 - **Flexible, fast and inexpensive process**

Reflectance recovery: proposed approach

- Reflection equation again:

$$B(\rho, \omega_0) = \int_{S^2} L(\omega_i) (\mathcal{R}(\rho)\Gamma)(\omega_i, \omega_0) d\Omega(\omega_i)$$

- **Solve the reflection equation directly**, under natural environmental illumination.
- Difficult inverse problem.
- **Shift the complexity** from elaborate experiment apparatus and procedures to more complicated algorithms but much simpler acquisition.
- Considered previously by Ramamoorthi & Hanrahan but limited to very low frequencies due to computational complexity → focused on **theoretical implications**.
- **Fast, spherical wavelet based methods**.
 - much higher frequencies computationally tractable
 - greater accuracy and performance
- Proposed acquisition system.
- Advantages of proposed acquisition system:
 - Fast acquisition
 - Standard apparatus
 - Acquisition performed in natural environment, *e.g.* on set/site (provided some conditions met)
 - **Flexible, fast and inexpensive process**